JOURNAL OF APPLIED ELECTROCHEMISTRY 24 (1994) 1267–1275

Electrocatalytic properties of doped nickel boride based electrodes for the hydrogen evolution reaction

J. J. BORODZIŃSKI, A. LASIA

Département de Chimie, Université de Sherbrooke, Sherbrooke, Québec, Canada, J1K 2R1

Received 18 January 1994; revised 11 April 1994

Amorphous nickel boride electrodes doped by small amounts of Rh, Ru, Co, Cr, Zn or Pt were studied for the hydrogen evolution reaction (HER) in 1 M NaOH solution at 70 °C. Steady-state galvanostatic measurements, a.c. impedance spectroscopy, X-ray diffraction and scanning electron microscopy were used. The properties of the pressed electrodes and the kinetic parameters of the HER were determined. The constant phase element model adequately describes the a.c. behaviour of these electrodes. It was found that the HER proceeds through the Volmer–Heyrovsky mechanism. An increase in catalytic properties was observed for materials doped with Rh, Ru and Co.

1. Introduction

Despite efforts undertaken in recent years [1, 2] the overall efficiency of cathodes and anodes for water electrolysis is not yet satisfactory. A very promising group of materials for the hydrogen (HER) and oxygen evolution reaction are amorphous alloys [3–24], usually prepared by a rapid solidification method. The HER has been investigated mostly on metallic glasses containing Ni, Co, Fe, Si, B and P. Electrochemical processes on these materials were rather slow as compared with crystalline materials [17, 24], but the performance could be significantly enhanced [10, 11, 19–22] by appropriate chemical pretreatment, for example, etching. However, it is not clear [9, 17, 24] which factor is more important in the overall reaction rate: lack of a long-range crystalline structure or highly developed surface area. The most promising electrode materials for water electrolysis may be borides and phosphides of some transition metals (Ni, Co, Fe, Cr) [25–34] which have been prepared using chemical techniques. Amorphous nickel boride produced in a reaction between borohydride and aqueous nickel salt is the best known member of this group. Chemical synthesis of this product leads to nanoparticles of $10 \sim 50$ nm [31]. This material [27] was also found to be an efficient catalyst in various organic reactions. Recently, the HER was studied on pressed mixtures of amorphous Ni_2B and Ni powder electrodes in alkaline solutions [34]. The catalytic properties of chemically obtained amorphous nickel boride can be changed by changing the preparation conditions, for example, rate of borohydride addition, initial concentration and cooling rate, etc. [27]. Moreover, the electrocatalytic properties can be changed by doping nickel boride with small amounts of other transition metals during the synthesis [25]. The purpose of this paper is to study the HER in alkaline solutions on amorphous nickel boride electrodes, doped with different transition metals, and to determine how modifications of the electrode preparation procedures can influence their electrochemical activity toward the HER.

2. Experimental details

Amorphous nickel boride, Ni_2B, was obtained by reduction of nickel acetate (Anachemia, 98%) with sodium borohydride (Aldrich, 98%) in alkaline aqueous solution. The previously published [27] procedure was modified; the borohydride to nickel molar ratio was changed from 3 to 6, borohydride addition time was increased to about 5–6 min and, as a result, the product structure was more reproducible. The black precipitated powder was washed a few times with water, filtered and finally the product was dried at 90 °C. The doped nickel borides were made in a similar manner, with adequate amounts of aqueous solutions of Ru, Rh, Cr, Pt, Zn and Co salts (Aldrich) added to the nickel acetate before synthesis. For Pt two additional methods of preparation were applied, in the first one the nickel boride powder was wetted by H_2PtCl_6 solution, dried and kept at 250 °C under H_2, in the second one H_2PtCl_6 was chemically reduced by formaldehyde on an aqueous suspension of Ni_2B.

Approximately 1 to 2 g of electrode material was placed in a cylindrical shaped stainless steel mould (radius 0.65 cm, height 2–3 mm, geometric surface area 1.33 cm^2) and pressed (at 8000 kg cm^{-2}). The powders pressed without any binders were mechanically stable during the experiments. The influence of addition of 10% of binders such as lanthanum polymer [35] and PTFE [36] on electrode performance and properties was also tested. Electrodes containing lanthanum phosphate polymer were sintered in an inert atmosphere after pressing and the influence of the sintering temperature on electrode properties was tested. The last step in the

0021-891X

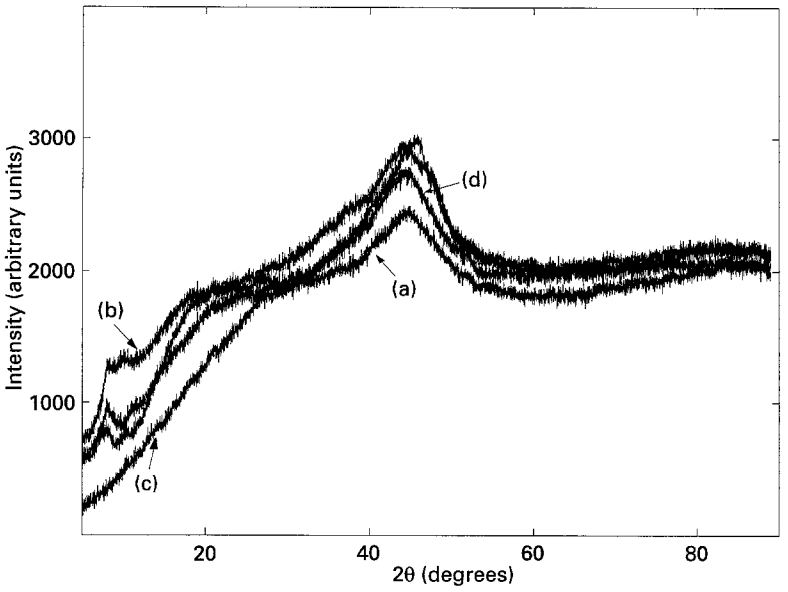

Fig. 1. X-ray spectra of nickel boride electrodes: (a) pure, (b) doped by 2% Ru, (c) 2% Cr and (d) 5% Zn.

electrode preparation consisted of attaching the electrical contact and insulating the walls and back of the electrode with alkaline resistive epoxy resin (Struers Epofix HQ). The electrical resistivity of electrodes, tested by a previously described method [36], was below 0.05 Ω cm except for those doped with molybdenum for which the resistance of a dry electrode was 50–100 Ω cm.

Electrochemical experiments were carried out in an H-type thermostated Pyrex glass cell with anodic and cathodic compartments separated by a Nafion® membrane (M-901 CATH/MD, DuPont). The measurements were carried out in 1 M NaOH solution (Aldrich 99.99%) at 70 °C (±0.1°C). Nickel foil served as a counter electrode and a Hg/HgO electrode in 1 M NaOH (25 °C) as a reference electrode; the latter was equipped with a Luggin capillary probe. The distance between the Luggin capillary and the working electrode centre was in the range of 1–2 mm, and the ohmic drop (measured by a.c. impedance method) was below 0.2 Ω. The potential of the Hg/HgO reference electrode measured against reversible hydrogen electrode in the investigated solution was equal to −913 mV. During the experiments nitrogen was passed through the cathodic and anodic compartments. All solutions were prepared with deionized water (Barnsted Nanopure). No special pretreatment of the electrodes was used, except for the electrodes doped by Zn and Cr, which were leached in 30% NaOH at 70 °C, using a procedure similar to that for Raney nickel based electrodes [37].

Electrochemical measurements were carried out using a Model 273A PAR potentiostat/galvanostat, Model 5210 PAR lock-in amplifier and 80286 based microcomputer connected via GPIB interface. All the electrochemical experiments consisted of two parts [36]. One hour after immersion of the electrodes in the solution 25 Tafel curves were measured galvanostatically in the current range 250 to 0.01 $\mu A\,cm^{-2}$ (5 s per point). Each Tafel curve measurement was followed by electrode conditioning for 30 min at 125 $mA\,cm^{-2}$). Then, a.c. impedance spectra (frequency range 10^4–5×10^{-3} Hz, a.c. amplitude 5 mV) were recorded. Standard PAR M388 software and our own program were used to control a.c. and d.c. experiments. All the measurements were corrected for ohmic drop.

3. Results and discussion

Transition metals Rh, Ru, Cr, Mo, V, Co, Zn and Pt were chosen as possible elements whose addition can increase electrocatalytic properties of nickel boride based electrodes. There are several reasons for such a choice. Electrocatalytic properties of metals such as Rh, Ru and Pt are well known. Electrodes made of pressed nickel powders with addition of small amounts of rhodium and ruthenium were found recently to be very active towards the HER [38, 39] and we expected similar behaviour in our case. An increase in catalytic properties of amorphous nickel borides doped with Cr, V, Co and Mo in hydrogenation of organic compounds [25] or in isopropanol dehydrogenation [26] was reported earlier.

Preliminary experiments confirmed that the morphology of the product depends strongly on the conditions of chemical synthesis. The average size of nickel boride particles (examined by scanning electron microscopy, SEM) can vary from 500 to 10 nm, the diameter of particles decreases with increase of the stirring intensity and with decrease of the rate of addition of borohydride to the reaction mixture. No evidence of a long-range crystalline order was found by the X-ray diffraction analysis, Fig. 1, where broad lines, characteristic for amorphous structures [31], were observed.

Doping metal quantities for all the electrodes were in the range of 0.5–10% wt/wt except for Pt, which was in the range of 0.1–0.5%. For small amounts of additives, the investigated material could be treated as structurally modified nickel boride. For higher doping concentrations, especially for elements with

properties different from nickel, a heterogenous mixture of borides with different physical and chemical properties were probably obtained. Similar properties were observed only for the borides of very closely related elements (like nickel and cobalt) [40]. In preliminary experiments it was also found that the electrochemical behaviour of borides doped by small amounts of vanadium or molybdenum were different from other materials studied. The electrodes obtained by pressing amorphous nickel boride powders doped with molybdenum were characterized by high internal electric resistance (50–100 Ω cm). Moreover, the resistance increased significantly when the electrodes were placed for a short time in alkaline solutions, even without the application of the electric current. This effect might arise from the surface passivation of powder particles through the formation of the molybdenum oxides. In fact, Divisek *et al.* [41] found that during the alkaline leaching molybdenum is removed from the surface. Besides, Tilak *et al.* [23] studying electrodeposited Ni–Mo–Cd electrodes found that the predominant form of molybdenum on the surface is MoO_3. They concluded that the surface is predominantly composed of layers of the nickel and molybdenum oxides. The doped amorphous nickel boride electrodes studied here are composed of consolidated nanoparticles [31] which might be covered on the surface by molybdenum oxides. These oxides probably have low electric conductivity which explains their high resistance. Besides, the chemical reduction might be not efficient enough to reduce molybdenum totally.

The vanadium doped electrodes had very poor mechanical stability and were usually destroyed after a few minutes of hydrogen evolution, however, they were not destroyed during soaking at an open circuit potential. Probably, the adherence of vanadium doped particles was lower and their structure permitted deeper penetration of electrolyte. As a result the internal pressure of evolving hydrogen destroyed the electrode. In consequence, both electrode materials (doped by Mo and V) were not further investigated.

The electrochemical activities of the electrodes were studied using steady-state galvanostatic polarization and a.c. impedance measurements. In Fig. 2, typical Tafel plots obtained for different materials are shown. Reproducible conditions in such galvanostatic experiments were obtained usually after registration of 2–5 curves. It is probably connected with the reduction of the surface oxides. In fact the colour of the electrodes changed during the HER from black to grey and then did not change after removal from the solution. In our earlier experiments with PTFE bonded nickel electrodes [36] much longer times were necessary in order to obtain reproducible Tafel curves. However, PTFE bonded electrodes are hydrophobic and the initial wetting process is much slower than for nickel boride based materials. Moreover, freshly prepared PTFE bonded nickel electrodes probably contain some organic impurities (from the stabilizing solution), which are slowly reduced or removed together with hydrogen evolution.

Exchange current densities, i_0, Tafel slopes, b, and overpotentials at current density equal to 250 mA cm^{-2}, η_{250}, were determined from log i against η plots and are displayed in Table 1. It is worth noting that a very well defined linear region with determination coefficient r^2 close to 0.9999 (least squares method) was normally observed for high current densities.

Tafel parameters are not sufficient to fully characterize the HER. Therefore, a.c. impedance measurements were carried out. For the majority of investigated electrodes made of doped nickel borides only one semicircle in the complex plane plot (Z'' against Z') was observed. Typical examples of complex plane and Bode plots are shown in Figs 3 and 4. The obtained data were fitted to a given model using a complex non-linear least-squares fitting

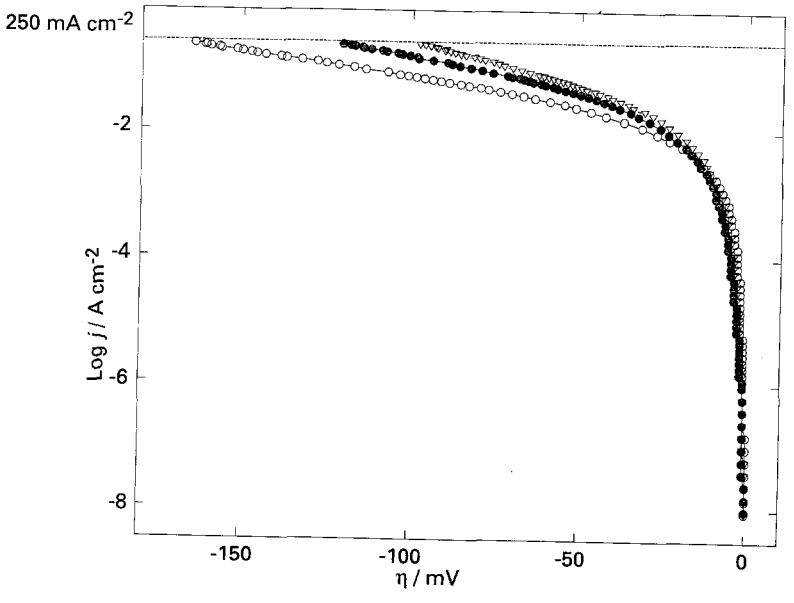

Fig. 2. Tafel plots for the HER in 1 M NaOH at 70 °C on nickel boride electrodes doped with (○) 0.1% Pt, (●) 0.5% Co and (▽) 2% Rh.

program (CNLS) [42–44]. For every experiment the experimental impedances were approximated with three different models: the one containing a constant phase element (CPE) instead of the double layer capacitance [45], the fractal model [46] and the porous electrode model [47]. The three models produce different shapes of the complex plane plots: the CPE model produces rotated semicircles, the fractal model deformed semicircles and the porous electrode model a straight line (at high frequencies) followed by a semicircle or a deformed semicircle. The fractal model with $\phi = 0.5$ is formally identical with the infinite pore model [47]. It was found that the CPE model fitted the best our experimental data and other models could be rejected on the basis of the statistical analysis [43]. The equivalent circuit consisted of the solution resistance, R_s, in series with the parallel connection of the constant phase element (CPE) and the faradaic impedance, Z_f [42]. The impedance of the CPE (Z_{CPE}) can be described as $Z_{CPE} = T^{-1}(j\omega)^{-\phi}$, where ω is the angular frequency of the a.c. signal, ϕ is the constant phase angle, and parameter T is related to double layer capacity (C_{dl}) and charge transfer resistance (R_{ct}) by the relation $T = C_{dl}^{\phi}(R_s^{-1} + R_{ct}^{-1})^{1-\phi}$ [45]. Results of the fitting of experimental impedances are also presented in Figs 3 and 4. Only for the electrodes doped with zinc (10 and 25%) did the infinite porous model [47] fit the experimental data better than the CPE. However, the kinetic parameters could not be determined because the pore parameters are not known.

The situation was more complicated for the electrodes made of nickel boride doped with Rh (8%), Co (8%), pure Ni_2B bonded by $LaPO_4$ (and sintered in 500 °C) and for mixtures of Ni_2B (doped by 2% of Rh and Ru) with nickel powder. In these cases two semicircles were observed (Fig. 5), the first at high frequencies was very small and overpotential independent, the second, much larger. The radius of the second semicircle decreased with increase of overpotential. Similar behaviour was observed recently for the HER on Ni–Zn [48] and Ni–Al [49] powder electrodes. The first semicircle is probably related to the electrode structure rather than to the electrochemical reaction (overpotential independent semicircle) [50]. Unfortunately, in the studied range of overpotentials the radius of the first semicircle was much smaller than that of the second one and it was impossible to determine its parameters precisely. The approximations in this case were performed assuming two circuits in series, each consisting of the parallel connection of the CPE and the resistance [48, 49]. Figure 5 presents typical Nyquist plots for such case, together with the approximated lines.

It is well established that the HER in alkaline solution may involve three following steps:

Volmer reaction

$$M + H_2O + e^- = MH + OH^- \quad (1)$$

Heyrovsky reaction

$$MH + H_2O + e^- = H_2 + M + OH^- \quad (2)$$

Tafel reaction

$$2MH = H_2 + 2M \quad (3)$$

The first step is the electrochemical reduction of water molecules with the formation of hydrogen adsorbed on the electrode surface. It is followed by the electrochemical and/or chemical desorption processes. In particular cases other factors like formation of hydrides or reactions with adsorbed species can also take part in the overall process. The reaction rates for the above processes can be described [51] by the following equations:

$$v_1 = k_1(1-\Theta)\exp(-\beta_1 f\eta) - k_{-1}\Theta\exp[(1-\beta_1)f\eta] \quad (4)$$

$$v_2 = k_2\Theta\exp(-\beta_2 f\eta) - k_{-2}(1-\Theta)\exp[(1-\beta_2)f\eta] \quad (5)$$

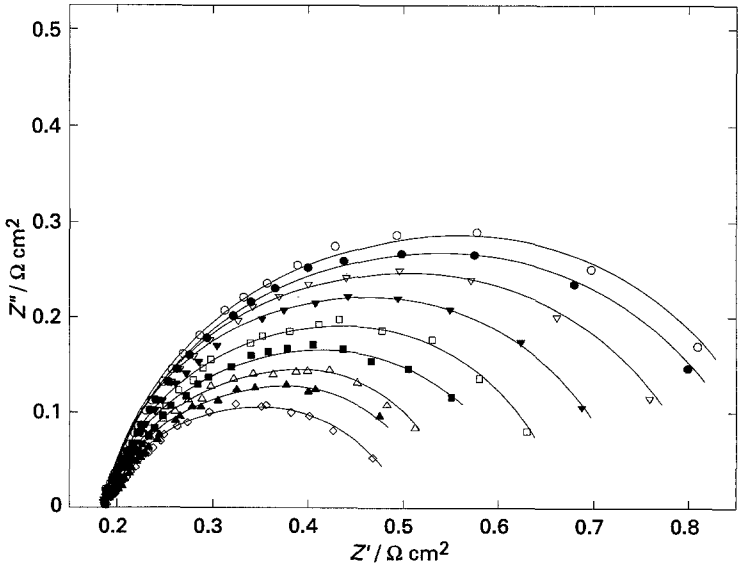

Fig. 3. Complex plane plots for nickel boride doped with Cr (2%) at different overpotentials: (○) 25, (●) 33, (▽) 42, (▼) 50, (□) 57, (■) 65, (△) 72, (▲) 79 and (◇) 86 mV. Points: experimental data; lines: values calculated according to the CPE model.

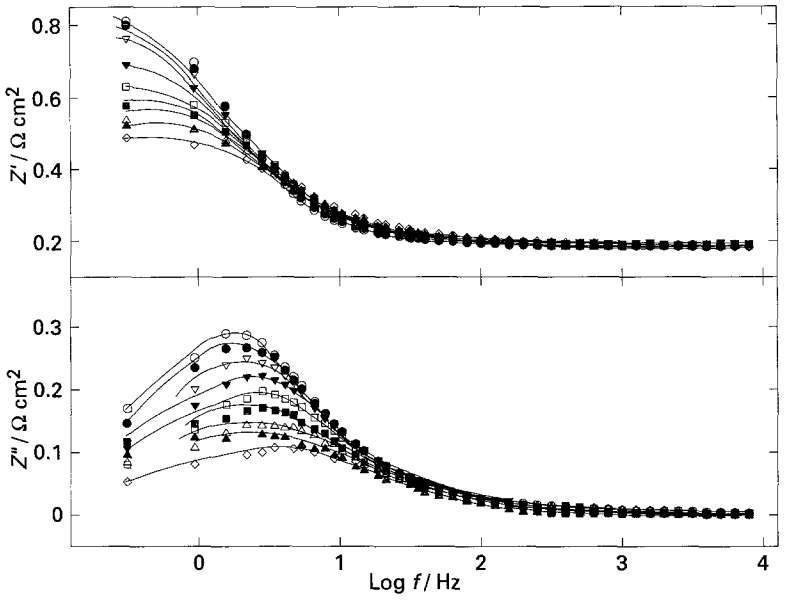

Fig. 4. Bode plots for nickel boride doped with Cr (2%) at different overpotentials: (○) 25, (●) 33, (▽) 42, (▼) 50, (□) 57, (■) 65, (△) 72, (▲) 79 and (◇) 86 mV. Points: experimental data; lines: values calculated according to the CPE model.

$$v_3 = k_3\Theta^2 - k_{-3}(1-\Theta)^2 \quad (6)$$

and the observed faradaic current equals:

$$i = F(v_1 + v_2) \quad (7)$$

At equilbrium: $v_1 = v_2 = v_3 = 0$ and the rate constants are related by the following equation:

$$k_1 k_2 k_{-1}^{-1} k_{-2}^{-1} = k_1^2 k_3 k_1^{-2} k_{-3}^{-1} = 1 \quad (8)$$

In the above equations β_1 and β_2 are the transfer coefficients for the Volmer and Heyrovsky steps, Θ is the surface coverage by adsorbed hydrogen, $f = F/RT$, v_i are the rates of corresponding reactions and k_i rate constants in mol cm^{-2} s^{-1}. Surface concentrations of OH^-, H_2 and H_2O are included in the rate constants and it is supposed that their changes during the reaction are negligible.

The above equations were used to determine the rate constants and the reaction mechanism. Current densities, obtained from steady-state polarization experiments, together with the charge transfer resistances from a.c. impedance measurements were fitted using the NLS program [42, 43]. In the calculations it was assumed that transfer coefficients for both electrochemical steps are equal to 0.5. It was found that for each investigated electrode the best approximation of experimental data could be obtained assuming the Volmer–Heyrovsky mechanism. Such a mechanism was also observed for the HER in alkaline media on other electrodes [35–42]. In Figs 6 and 7 the experimental values of R_{ct} and current densities are compared with those found using the NLS fit. Table 1 presents values of the rate constants (k_1), Tafel parameters, constant phase angles and double layer capacities. For the Volmer–Heyrovsky mechanism it is impossible to distinguish the rate determining step on the basis of the electrochemical measurements [42] because two equivalent solutions exist and the kinetic parameters obtained are permutable. In Table 1 it was supposed that the Volmer reaction is the rate determining step (r.d.s.). The smallest rate constant (k_1) only is presented because

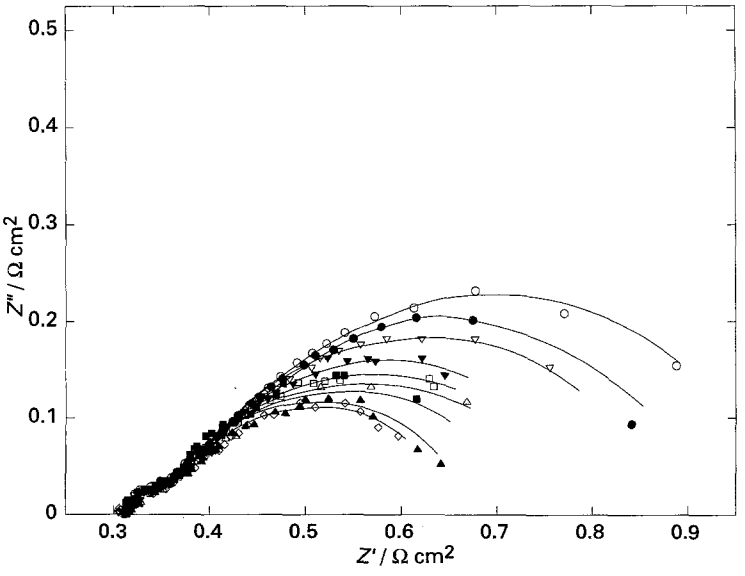

Fig. 5. Complex plane plots for nickel boride electrodes doped with Co (8%) at different overpotentials: (○) 33, (●) 40, (▽) 47, (▼) 54, (□) 60, (■) 67, (△) 74, (▲) 79 and (◇) 85 mV. Points: experimental data; lines: values calculated according to the CPE model.

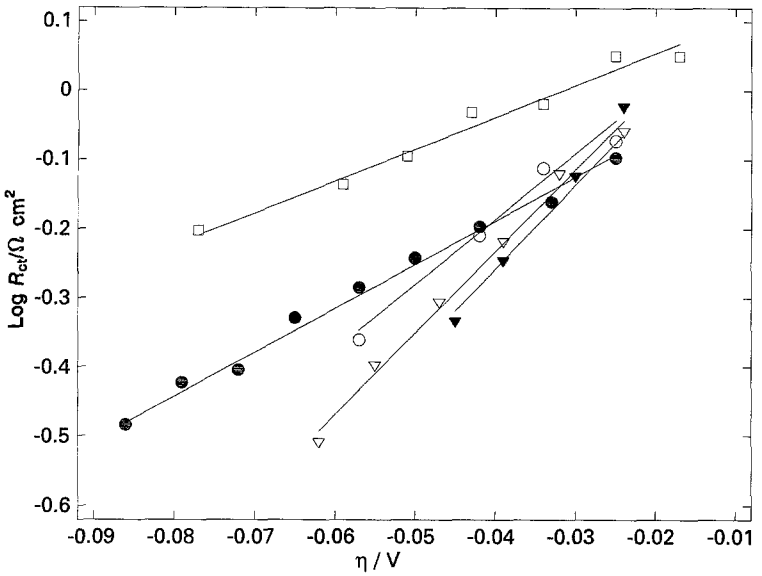

Fig. 6. Charge transfer resistances for the nickel boride electrodes as function of overpotentials. Points: experimental; lines: calculated according to the Volmer–Heyrovsky model. Electrode materials doped with (○) 2% Co, (●) 2% Cr, (▽) 2% Rh, (▼) 2% Ru and (□) 2% Zn.

the errors of the other rate constants were larger than their values.

The range of overpotentials available for a.c. experiments was rather narrow (~ 100 mV) because a vigorous hydrogen evolution affected the measurements. In this potential range changes in the double layer capacitance (C_{dl}) and constant phase angle (ϕ) were practically negligible. The values of C_{dl}, observed in most cases, were in a range of 0.25–0.6 F cm^{-2} and the constant phase angles in a range 0.6–0.8. Assuming the double layer capacitance of a smooth metal surface as equal to 20 μF cm^{-2} [52] the roughness factor $R = C_{dl}/20\,\mu\text{F cm}^{-2}$ is of the order of 10^4. Such values are reasonable for moderately irregular, porous surfaces [53]. It was found earlier [38, 54, 55] that the porosity of electrode materials (expressed here by roughness factor) calculated from C_{dl} data is in good agreement with values obtained from the non-electrochemical BET method.

For the electrodes made of nickel borides doped by zinc (for higher Zn contents) larger C_{dl} values and lower constant phase angles were observed. This behaviour is probably related to the more porous structure of the boride. During the chemical reduction of metal salts two competitive reactions take place [56]:

$$4M^{2+} + BH_4^- + 8OH^- \longrightarrow 4M + BO_2^- + 6H_2O \quad (9)$$

$$4M^{2+} + 2BH_4^- + 6OH^- \longrightarrow 2M_2B + 6H_2O + H_2 \quad (10)$$

For Ni, Co and Fe salts the second reaction is predominant [32] and compounds with stoichiometric M : B = 2 : 1 ratio were obtained. But for other metals it is possible that the first process can also take place leading to the incorporation of metallic zinc into the structure. Subsequent leaching of zinc or zinc boride in alkaline solution would lead to a larger surface roughness. To avoid uncontrollable changes of the electrode structure in alkaline solutions the electrodes made of nickel borides doped by Zn and Cr were leached in 30% NaOH for a few hours before the experiment. In the case of zinc doped electrodes gas evolution from the elec-

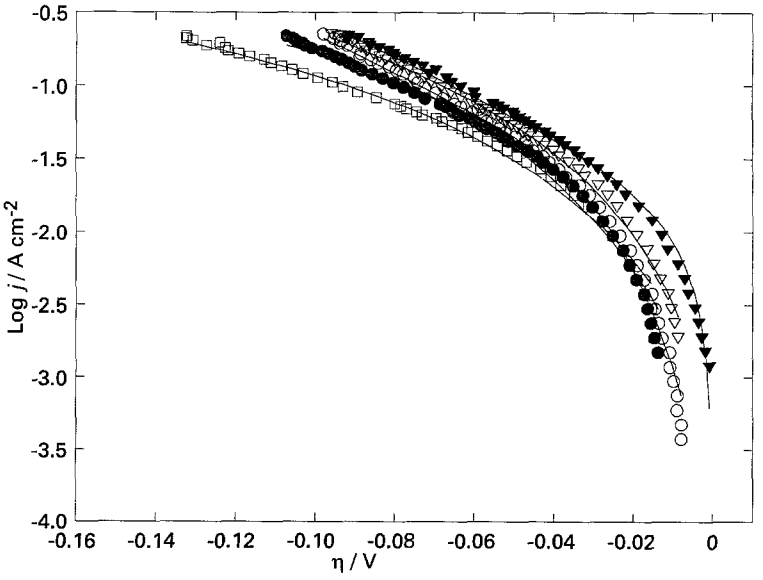

Fig. 7. Current densities for the HER on the nickel boride doped electrodes as function of overpotentials. Points: experimental; lines: calculated according to the Volmer–Heyrovsky model. Electrode materials doped with (○) 2% Co, (●) 2% Cr, (▽) 2% Rh, (▼) 2% Ru and (□) 2% Zn.

Table 1. Electrochemical parameters for the HER on doped nickel boride electrodes in 1 M NaOH at 70 °C

Addition to nickel boride	η_{250} /mV	*Slope* /mV	j_0 /mA cm^{-2}	ϕ	C_{dl} /F cm^{-2}	k_1 /mol cm^{-2} s^{-1}
none	133	85	5.9	0.77 ± 0.11	0.30	1.05 ± 0.04
2.0% Cr	112	81	11	0.80 ± 0.02	0.52	2.51 ± 0.04
0.1% Pt	160	126	14	0.59 ± 0.03	0.24	0.93 ± 0.42
0.3% Pt	141	119	16	0.61 ± 0.02	0.25	1.14 ± 0.13
0.5% Pt	133	93	9.3	0.66 ± 0.02	0.80	1.33 ± 0.02
0.5% Co	126	100	14	0.68 ± 0.03	0.37	1.77 ± 0.08
2.0% Co	100	68	8.7	0.80 ± 0.06	0.82	2.61 ± 0.09
8.0% Co	127	111	18	0.68 ± 0.04	0.51	3.11 ± 0.12
0.5% Rh	127	102	14	0.62 ± 0.04	0.35	1.77 ± 0.06
2.0% Rh	96.5	69.2	10	0.81 ± 0.06	0.61	2.87 ± 0.08
8.0% Rh	117	130	31	0.73 ± 0.06	0.41	1.79 ± 0.18
0.5% Ru	112	90	15	0.60 ± 0.03	0.32	1.86 ± 0.06
2.0% Ru	94	72	13	0.63 ± 0.04	0.47	2.71 ± 0.10
8.0% Ru	75	89	39	0.61 ± 0.02	0.46	3.64 ± 0.17
2.0% Zn	139	112	15	0.71 ± 0.02	0.39	2.23 ± 0.06
5.0% Zn	123	117	22	0.55 ± 0.05	1.7	2.52 ± 0.23
10.0% Zn	140	139	25	0.69 ± 0.04	*	*

* Could not be determined because the pore parameters are not known.

trode surface was observed during the leaching process.

Data presented in Table 1 reveal that a moderate enhancement of electrocatalytic properties is induced by doping nickel boride with Ru, Rh, Co and Cr. For Pt and Zn doped electrodes electrocatalytic properties remained practically unchanged or became worse.

Two main effects influence the electrocatalytic properties of the electrodes. First, foreign metal incorporated into the nickel boride structure can create heterogenous sites characterized by different activity. In consequence, metals with higher electrocatalytic activity toward the HER should enhance overall electrode properties. This can explain the increase of kinetic parameters for Rh and Ru doped materials. Moreover, metals like Co and Cr could not cause any changes in electrode behaviour. Second, the metals introduced during the chemical synthesis can modify the surface structure of Ni_2B microparticles, rather than create heterogenous sites. Higher values of C_{dl} and lower constant phase angles of doped borides suggest that the surface structure is probably more developed. A similar explanation of the increase of nickel boride catalytic properties after promotion by a small amount of chromium was suggested earlier [26]. The electrocatalytic properties of the investigated materials, similar to those of chemically etched amorphous glasses, are results of highly developed homogenous structure rather than of heterogenous catalysis.

The low activity of the platinum doped nickel boride may be explained by formation of a homogenous platinum boride dispersed in Ni_2B without formation of active surface clusters. Other methods of platinum deposition such as chemical reduction of H_2PtCl_6 on Ni_2B particles in water suspension by formaldehyde or reduction of H_2PtCl_6 solution on

Table 2. Electrochemical parameters for the HER on modified nickel boride electrodes in 1 M NaOH at 70 °C

Electrode	η_{250} /mV	*Slope* /mV	j_o /mA cm^{-2}	ϕ	C_{dl} /F cm^{-2}	k_1 /mol cm^{2} s^{-1}
90% Ni–B, 10% Ni (2.0% Rh in Ni–B)	93	65.2	9.4	0.80 ± 0.02	0.44	2.66 ± 0.07
90%Ni–B, 10% Ni (2.0% Ru in Ni–B)	104	80	13	0.79 ± 0.05	0.48	2.34 ± 0.05
Ni–B sintered at 400 °C	120	115	23	0.58 ± 0.21	0.12	2.53 ± 0.12
Ni–B sintered at 600 °C	140	153	31	0.60 ± 0.04	0.045	1.28 ± 0.06
Ni–B sintered at 800 °C	354	220	6.0	0.60 ± 0.06	0.0022	0.0747 ± 0.0150
Ni–B + 10% PTFE pressed at room temperature	250	161	6.2	0.73 ± 0.14	0.10	0.106 ± 0.013
Ni–B with 10% $LaPO_4$ sintered at 300 °C	118	108	20	0.70 ± 0.01	0.27	2.74 ± 0.09
Ni–B with 10% $LaPO_4$ sintered at 500 °C	171	156	20	0.80 ± 0.02	0.15	0.977 ± 0.763

Ni_2B by a stream of hydrogen at 300 °C also produced electrodes of poor activity ($\eta_{250} \approx 200$ mV).

It was found earlier [34] that mixing amorphous nickel boride and nickel powders (90 : 10%) increased activity toward the HER. The results presented in Table 2 show no evidence of an increase in activity. However, the powders reported in this paper were obtained using a modified procedure.

The electroactive materials may also be bound with inorganic polymer $LaPO_4$ [35] but the polymerization takes place at higher temperatures. According to the data presented in Table 2, such a process decreases the electrode performance toward the HER if the sintering temperature is higher than 400 °C. There are two possible reasons for such behaviour: the real surface electrode area may decrease and the structure may become more crystalline. Decrease of double layer capacity suggests that the average surface area and roughness factor are lower for the sintered electrodes. However, data presented in Table 2 indicate that despite the fact that k_1 decreases, the intrinsic rate constants (k_1/surface roughness) increase with the sintering temperature. This observation indicates that as the surface area decreases crystallization takes place and more active reaction sites are formed.

4. Conclusions

Studies of the HER on nickel boride electrodes doped by Rh, Ru, Co, Cr, Zn and Pt carried out by quasi steady-state galvanostatic experiments and by a.c. impedance spectroscopy show that the overall electrode reaction proceeds via the Volmer–Heyrovsky mechanism. The reaction rates, as compared to those of the pure nickel boride electrode, increase for electrodes doped with Rh, Ru, Cr and Co but are the same or even worse for those doped with Pt and Zn. The materials obtained have a large surface area which is the main reason of their activity. The presence of more active centres does not change significantly the overall performance. Sintering at higher temperatures during the electrode preparation causes a decrease in activity for the HER. The sintering process causes a decrease of the real surface and partial transfer from amorphous to crystalline structure. The a.c. behaviour may be explained by the constant phase element model. The electrode materials have good mechanical and physical properties and long term stability.

Acknowledgements

The financial support from the Ministère de l'Energie et de Ressources du Québec (Chair on Hydrogen) is gratefully acknowledged.

References

[1] H. Wendt and G. Imarisio, *J. Appl. Electrochem.* **18** (1988) 1.
[2] S. Trasatti *in* 'Advances in Electrochemical Science and Engineering', Vol. 2 (edited by H. Gerischer and W. Tobias), VCH, New York (1992) p. 1.
[3] J. J. Gilman, *Science* **208** (1980) 856.
[4] D. Turnbull, *Metall. Transact.* **12B** (1980) 217.
[5] W. E. Brower Jr., S. Matyjaszczyk, T. L. Pettit and G. V. Smith, *Nature* **301** (1983) 497.
[6] C. Yoon and D. L. Cocke, *J. Non-Cryst. Solids* **79** (1986) 217.
[7] D. L. Cocke, E. D. Johnson and R. P. Merril, *Catal. Rev. Sci. Eng.* **26** (1984) 163.
[8] K. Hashimoto, 'Passivity of Metals and Semiconductors', Proc. 5th Int. Symp. (1983) 235.
[9] M. D. Archer, C. C. Corke and B. H. Harji, *Electrochim. Acta* **32** (1987) 13.
[10] G. Kreysa and B. Håkansson, *J. Electroanal. Chem.* **201** (1986) 61.
[11] G. Kreysa, J. Gomez, A. Baro and A. J. Arvia, *ibid.* **265** (1989) 67.
[12] H. Alemu and K. Jüttner, *Electrochim. Acta* **33** (1988) 1101.
[13] K. Lian, D. W. Kirk and S. J. Thorpe, *ibid.* **36** (1991) 537.
[14] *Idem, ibid.* **37** (1992) 169.
[15] *Idem, ibid.* **37** (1992) 2029.
[16] N. C. Grant and M. D. Archer, *J. Electrochem. Soc.* **131** (1984) 997.
[17] K. Seto, J. Noël, J. Lipkowski, Z. Altounian and R. Reeves, *ibid.* **136** (1989) 1910.
[18] G. Tremiliosi-Filho, E. R. Gonzalez, S. Srinivasan and A. J. Appleby, *J. Electroanal. Chem.* **331** (1992) 751.
[19] K. Machida, M. Enyo, K. Kai and K. Suzuki, *J. Less-Common Met.* **100** (1984) 373.
[20] K. Machida and M. Enyo, *Bull. Chem. Soc. Japan* **58** (1985) 2043.
[21] M. Enyo, T. Yamazaki, K. Kai and K. Suzuki, *Electrochim. Acta* **28** (1983) 1573.
[22] K. Machida, M. Enyo, Y. Toyoshima, K. Miyahara, K. Kai and K. Suzuki, *Bull. Chem. Soc. Japan* **56** (1983) 3393.
[23] B. V. Tilak, A. C. Ramamurthy and B. E. Conway, *Proc. Indian. Acad. Sci. (Chem. Sci.)* **97** (1986) 359.
[24] M. Naka, K. Hashimoto, T. Masumoto and I. Okamoto, Proc. 4th Int. Conf. on *Rapidly Quenched Metals* (edited by T. Masumoto and K. Suzuki), Japan Institute of Metals, Sendai (1982) 1431.
[25] R. Paul, P. Buisson and N. Joseph, *Ind. Eng. Chem.* **44** (1952) 1007.
[26] D. Mears and M. Boudart, *AIChE J.* **12** (1966) 312.
[27] Ch. Brown, *J. Org. Chem.* **35** (1970) 1900.
[28] F. Nozaki and R. Adachi, *J. Catal.* **40** (1975) 166.
[29] R. C. Wade, D. G. Holar, A. N. Hughes and B. C. Hui, *Catal. Rev.* **14** (1976) 211.
[30] J. van Vonterghem, S. Morupm, Ch. Koch, S. Charles and S.Wells, *Nature* **322** (1986) 622.
[31] J. Saida, A. Inoue and T. Masumoto, *Metal. Trans.* **22A** (1991) 2125.
[32] J. Saida, A. Inoue and T. Masumoto, *Mater. Sci.* **A133** (1991) 771.
[33] S. Yoshida, H. Yamashita, T. Funabiki and T. Yonezawa, *J. Chem. Soc., Chem. Commun.* (1982) 964.
[34] P. Los and A. Lasia, *J. Electroanal. Chem.* **333** (1992) 115.
[35] H. Dumont, P. K. Wrona, J. M. Lalancette, H. Ménard and L. Brossard, *J. Appl. Electrochem.* **22** (1992) 1049.
[36] J. J. Borodziński and A. Lasia, *Int. J. Hydrogen Energy* **18** (1993) 985.
[37] Y. Choquette, L. Brossard, A. Lasia and H. Ménard, *Electrochim. Acta* **35** (1990) 1251.
[38] H. Dumont, P. Los, L. Brossard, A. Lasia and H. Ménard, *J. Electrochem. Soc.* **139** (1992) 2143.
[39] *Idem, J. Appl. Electrochem.* **23** (1993) 684.
[40] J. J. Borodziński and A. Lasia, unpublished results (1993).
[41] J. Divisek, H. Schmitz and J. Balej, *J. Appl. Electrochem.* **19** (1980) 519.
[42] A. Lasia and A. Rami, *J. Electroanal. Chem.* **294** (1990) 123.
[43] P. Wrona, A. Lasia, M. Lessard and H. Ménard, *Electrochim. Acta* **37** (1992) 1283.
[44] J. R. Macdonald, J. Schoonman and A. P. Lehner, *J. Electroanal. Chem.* **131** (1982) 77.
[45] G. J. Brug, A. L. G. van der Eeden, M. Sluyters-Rehbach and J. H. Sluyters, *ibid.* **176** (1984) 275.
[46] L. Nyikos and T. Pajkossy, *Electrochim. Acta* **30** (1985) 1533.
[47] P. Los, A. Lasia, L. Brossard and H. Ménard, *J. Electroanal. Chem.* **360** (1993) 101.

[48] L. Chen and A. Lasia, *J. Electrochem. Soc.* **139** (1992) 3214.
[49] L. Chen and A. Lasia, *ibid.* **140** (1993) 2464.
[50] H. Keiser, K. D. Beccu and M. A. Gutjahr, *Electrochim. Acta* **21** (1976) 539.
[51] A. Lasia and A. Rami, *J. Electroanal. Chem.* **294** (1990) 123.
[52] S. Trassati and O. A. Petrii, *Pure Appl. Chem.* **63** (1991) 711.
[53] A. Lasia, *Int. J. Hydrogen Energy* **18** (1993) 557.
[54] Y. Choquette, A. Lasia, L. Brossard and H. Ménard, *J. Electrochem. Soc.* **137** (1990) 1723.
[55] L. Chen and A. Lasia, *ibid.* **138** (1991) 3321.
[56] I. Dragieva, M. Slavcheva and D. Buchkov, *J. Less-Common Met.* **117** (1986) 317.